Journal of Marine Science and Application (2022) 21: 37-50
https://doi.org/10.1007/s11804-022-00253-2

RESEARCH ARTICLE

Wave Scattering by a Submerged Sphere in Three-Layer Fluid

Minakshi Ghosh, Manomita Sahu and Dilip Das

Received: 21 September 2021 / Accepted: 04 January 2022

Abstract
Using linear water wave theory, three-dimensional problems concerning the interaction of waves with spherical structures in a fluid which contains a three-layer fluid consisting of a layer of finite depth bounded above by freshwater of finite depth with free surface and below by an infinite layer of water of greater density are considered. In such a situation time-harmonic waves with a given frequency can propagate with three wavenumbers. The sphere is submerged in either of the three layers. Each problem is reduced to an infinite system of linear equations by employing the method of multipoles and the system of equations is solved numerically by standard technique. The hydrodynamic forces (vertical and horizontal forces) are obtained and depicted graphically against the wavenumber. When the density ratio of the upper and middle layer is made to approximately one, curves for vertical and horizontal forces almost coincide with the corresponding curves for the case of a two-layer fluid with a free surface. This means that in the limit, the density ratio of the upper and middle layer goes to approximately one, the solution agrees with the solution for the case of a two-layer fluid with a free surface.

Keywords Three-layer fluid; Wave scattering; Submerged sphere; Hydrodynamic forces; Vertical and horizontal forces; Linear water wave theory; Density-stratified three-layer fluid; Submerged spherical structure; Underwater sphere

1 Introduction

The study of wave propagation problems concerning fully submerged or semi-immersed structures of spherical shape within the fluid has been essential and received immense importance in the literature for their utilization as wave power devices or as a spherical hull in submerged vehicles and others. Havelock (1955) initiated the study of spheres in the fluid, who investigated the radiation by a half-immersed heaving sphere in deep water and solved the problem considering the velocity potential as a summation of wave source potentials of three-dimension and harmonic wave-free potentials taken in a linear combination. This method was used by Evans and Linton (1989) in the water of finite depth to study scattering and radiation by submerged horizontal cylindrical structure. Extending this in a similar approach, Linton (1991) dealt with the case of a submerged spherical object. The multipole expansion method has made a prime place in the study of various hydrodynamic characteristics of different geometries that are complaint to separable solutions of Laplace's equation. This method was practised initially by Ursell (1950) to study waves considering the presence of a submerged long horizontal circular cylinder in the water of infinite depth. Srokosz (1979) used the method of multipoles for the radiation problem of water waves by a sphere, considering it as a wave power absorber fully submerged in deep water under a free surface. Many researchers, including Das and Mandal (2008; 2010) have worked on problems of hydrodynamic concerns, analysing fixed rigid spherical structures. Das and Thakur (2013) analysed the problem of wa-

Article Highlights

- The sphere is considered to be submerged in either the lower, the middle or the upper layer of the three-layer fluid.
- The method of multipoles expansion has been used.
- Analytical expressions for hydrodynamic forces are obtained for each problem when the sphere is submerged in either layer of the fluid.
- The horizontal and vertical forces are acquired analytically as well as numerically.
- The obtained results for each problem are represented graphically against the wavenumbers and have been studied.

✉ Dilip Das
dilipdas99@gmail.com

[1] Department of Mathematics, Diamond Harbour Women's University, Sarisha 743368, India

ter wave scattering in the presence of a submerged sphere considering a thin ice-cover as an elastic plate in the water of uniform finite depth, and that in a two-layer fluid was investigated by Das and Thakur (2014), applying the method of multipoles. Such studies emphasize spherical shape devices of wave energy in oceans of polar regions. Most of the research works are concerned with completely immersed spherical objects. There are rare researchers on spheroids, a more complex geometry (cf. Wu and Taylor (1987; 1989), Chatjigeorgiou (2013), Chatjigeorgiou and Miloh (2015; 2017), and others.)

Geophysical flows of oceans and atmosphere have an essential feature of density inhomogeneity, due to which there can be significant effects in the dynamics of the flow. Density stratification in the fluid flows of nature and industrial processes are due to the differences in salinity, the concentration of several solutes, temperature, and their combination. Estuaries or fjords have fresh river water flowing over oceanic saline water. Even though almost all fluids in the earth are stratified, the effects of density stratification of seawater were not considered in the initial researches, and an assumption of fluids of uniform density was usual. A general theory of propagation of water waves in a density stratified fluid of two layers with a free surface was developed by Linton and McIver (1995), considering the presence of long horizontal cylindrical structures in either of the two layers. This study was motivated by the model of underwater pipe bridges across the stratified fluid of Norwegian fjords where the freshwater of around 10m depth flows over the saltwater. Extending this research, Cadby and Linton (2000) investigated the three-dimensional scattering and radiation problem in the presence of a submerged sphere in any of the two layers, using the multipole expansion method. Interesting flows of polar oceans were studied considering the more general class of problems of the density stratified two-layer fluid with ice cover or floating thin elastic plate (cf. Das (2008; 2015), Das and Mandal (2006; 2007)). In the same fluid structure, the radiation of water waves by a sphere was investigated by Das and Mandal (2010). Recently, Sahu and Das (2021) studied the hydrodynamic forces on a submerged circular cylinder in two-layer fluid with an ice-cover.

We also know that based on the layered density structure, the ocean has three horizontal depth zones, namely, the mixed layer, pycnocline, and deep layer. Severe density changes take place in pycnocline. The density gradients may occur by the gravitational settling of sediments or solar heating of the surface water and also as a result of minimal mixing forces of wind and wave action, which is more often in the summer months. In recent years, the study of stratified fluid dynamics has drawn more attention, understanding the vital effect of inhomogeneity of density in ocean engineering applications (cf. Liu et al. (2020); Wang et al. (2021) and others). In a three-layer fluid model with a free upper surface and two interfaces, the water wave propagates with three possible modes of linear water waves, each with different wavenumbers. This fact makes the model mathematically difficult to handle. Each of the three modes may correspond to the oscillations confined mainly to the upper, middle and lower layer of fluid, respectively. In interaction with the body in the wave field of stable but arbitrary density ratio, the wave energy may have a chance of transferring from one mode to another. Hence, this model is considered a more accurate realization of the two-layer fluid model. There are published research works in three-layer fluid with some fascinating results to understand wave interaction with different geometrical configurations for some particular interests. The water wave in a three-layer system containing rigid horizontal walls above the top layer and below the bottom layer of fluid was investigated by Michallet and Dias (1999). Taylor (1931) studied the linear stability of a three-layer fluid. The trapped modes of wave in such fluid in a channel with a fully immersed cylinder in the lower layer fluid was discussed by Chakrabarti et al. (2005). Also, Chen and Forbes (2008) studied steady periodic waves considering shear in the middle layer of the three-layer fluid. Problems of wave structure interaction in the three-layer fluid were discussed by Mondal and Sahoo (2014). Less work has been done in this regard. Das (2016) investigated the scattering of water waves by horizontal cylindrical structure in a three-layer fluid. Recently, oblique wave scattering in the three-layer fluid was studied by Das and Majumder (2020) using the method of multipoles expansion. Newly, Das and Sahu (2021) investigated wave radiation by a sphere in a three-layer fluid.

Solution of relevant fluid mechanics problems is paramount to understand flows of interest in oceanography and construct advanced necessary off-shore structures like submerged sphere-city, called ocean spiral. In Naval hydrodynamics, experimental and numerical tools are used to study the flow field around marine vessels. Underwater models of spherical robots are analysed for their various utilisation in ocean phenomena (cf. Amran and Isa 2020). Studies of autonomous underwater vehicles (AUVs) of spherical structure is of major use for mine exploration (cf. Fernandez et al. 2018 and others). Lately, Gu et al. (2021) used a heaving spherical wave energy converter (WEC) as a point absorber to test their proposed controller. Freshly, Samayam et al. (2021) considered an oscillating sphere close to a plane boundary to investigate direct numerical simulation (DNS) of flow induced by it. Most of their review reveals that ignoring the effects of density stratification, fluid is taken to be of uniform density. The submerged spherical structure in a three-layer fluid can be studied to inspect vital problems regarding interesting ocean hydrodynamic phenomena, making the investigation more realistic. This three-dimen-

sional body can resemble spherical submarines, various wave energy devices, subsurface storage tanks, or fuel bladder of spherical geometric configuration in the ocean. Moreover, the spheroidal structures of vehicles fixed within the ocean are also being studied. The scattering of water waves in a three-layer fluid in the presence of a submerged sphere in any one of the three layers is examined here. The focus is on the quantity of wave energy reflected and transmitted due to the obstruction of the incident wave by the spherical structure and thus calculating the resultant vertical and horizontal forces. This information is essential for the stable and efficient construction of immersed bodies having sphere shapes in the ocean. The method of multipole expansions is employed to express the velocity potentials in spherical harmonics that describe the motion in either of the three layers. Applying the structural boundary conditions of the surface of the submerged sphere, the problem is reduced to a system of linear algebraic equations. These equations are truncated and simultaneously solved using numerical methods. Finally, the vertical and horizontal exciting forces on the sphere are obtained respectively for the heave and sway motions of the submerged body. These forces for the structure submerged in either lower, middle or upper layer are depicted graphically against the wave number in several figures, varying the submersion depth of the sphere. The curves are almost similar to those of Cadby and Linton (Cadby and Linton 2000) when the densities of the upper and the middle layer of the three-layer fluid are nearly equal, as the fluid represents only two layers.

2 Mathematical formulation

It is concerned with irrotational motion in three superposed non-viscous incompressible fluids under the action of gravity and neglecting any effect due to surface tension at the interfaces. H and h are the depths of the upper and the middle layer respectively, while the lower layer is infinitely deep. The densities of the upper, middle and lower layers are ρ_1, ρ_2 and $\rho_3\,(\rho_3 > \rho_2 > \rho_1)$ respectively. Cartesian co-ordinates are chosen such that (x, z) plane coincides with the undisturbed interface between the middle and lower layer (ML). The y- axis points vertically upwards with $y = 0$ as the mean position of the interface of ML, $y = h\,(>0)$ as the mean position of the interface of the upper and middle (UM) and $y = H + h\,(>0)$ as the mean position of the linearized free surface. Under the usual assumptions of linear water wave theory, a velocity potential can be defined for waves in the form

$$\Phi(x, y, z, t) = \mathrm{Re}\left\{\phi(x, y, z)\,\mathrm{e}^{-\mathrm{i}\omega t}\right\}$$

where $\phi(x, y, z)$ is a complex valued potential function, ω is the angular frequency.

The upper fluid, $h < y < h + H$, will be referred to as region I, the middle fluid, $0 < y < h$, will be referred to as region II, while the lower fluid, $y < 0$, will be referred to as region III (cf. Figure 1(a), 1(b), 1(c)).

The potential in the upper fluid will be denoted by ϕ^{I} and that in the middle and lower fluids by $\phi^{\mathrm{II}}, \phi^{\mathrm{III}}$ respectively, $\phi^{\mathrm{I}}, \phi^{\mathrm{II}}$ and ϕ^{III} satisfied Laplace's equation (cf. Das and Sahu 2021)

$$\nabla^2\phi^{\mathrm{I}} = \nabla^2\phi^{\mathrm{II}} = \nabla^2\phi^{\mathrm{III}} = 0 \tag{1}$$

Linearized boundary conditions on the interfaces and at the free surface are

$$\phi_y^{\mathrm{I}} = \phi_y^{\mathrm{II}} \text{ on } y = h \tag{2}$$

$$s_1\left(\phi_y^{\mathrm{I}} - K\phi^{\mathrm{I}}\right) = \phi_y^{\mathrm{II}} - K\phi^{\mathrm{II}} \text{ on } y = h \tag{3}$$

$$\phi_y^{\mathrm{II}} = \phi_y^{\mathrm{III}} \text{ on } y = 0 \tag{4}$$

$$s_2\left(\phi_y^{\mathrm{II}} - K\phi^{\mathrm{II}}\right) = \phi_y^{\mathrm{III}} - K\phi^{\mathrm{III}} \text{ on } y = 0 \tag{5}$$

where $s_1 = \dfrac{\rho_1}{\rho_2}(<1)$ and $s_2 = \dfrac{\rho_2}{\rho_3}(<1)$

$$\left(\phi_y^{\mathrm{I}} - K\phi^{\mathrm{I}}\right) = 0 \text{ on } y = h + H \tag{6}$$

where $K = \omega^2/g$. The boundary conditions (2) and (4) are obtained from the continuity of normal velocity at the interface between UM and ML respectively, while the conditions (3) and (5) are obtained from the continuity of pressure at the interface between UM and ML respectively.

Also, condition at large depth is

$$\nabla\phi^{\mathrm{III}} \to 0 \text{ as } y \to -\infty \tag{7}$$

Now the total potential function can be decomposed into two parts:

$$\phi = \phi_{\mathrm{inc}} + \phi_s \tag{8}$$

where ϕ_{inc} is the incident wave potential function and ϕ_s is scattering potential function which must satisfy Equation (1) to (7) and also the body boundary condition

$$\frac{\partial\phi_s}{\partial r} = -\frac{\partial\phi_{\mathrm{inc}}}{\partial r} \text{ on } r = a \tag{9}$$

and behave as an outgoing wave far from the sphere. Without loss of generality, it can be assumed that the incident wave is from $x = -\infty$ so that $\alpha_{\mathrm{inc}} = 0$.

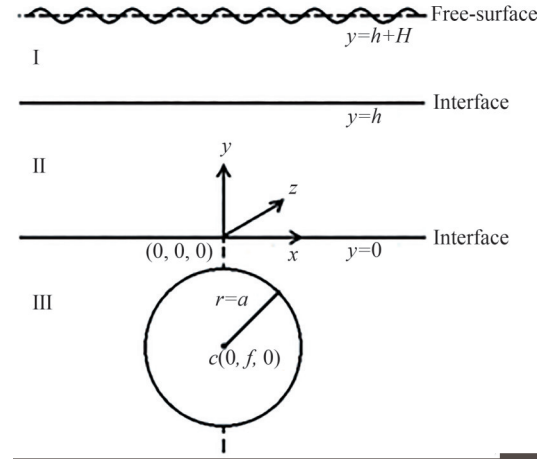

(a) Sphere submerged in the lower layer

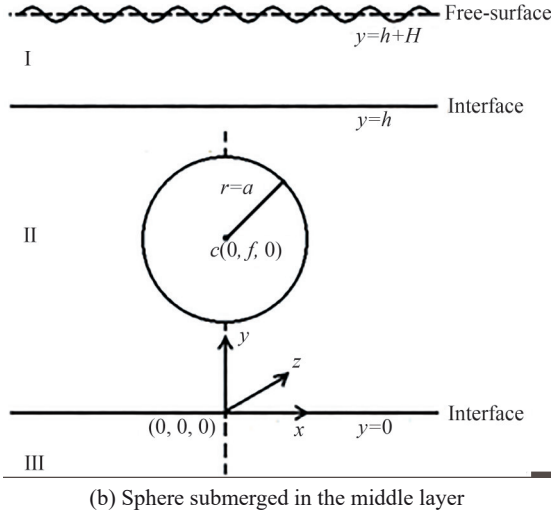

(b) Sphere submerged in the middle layer

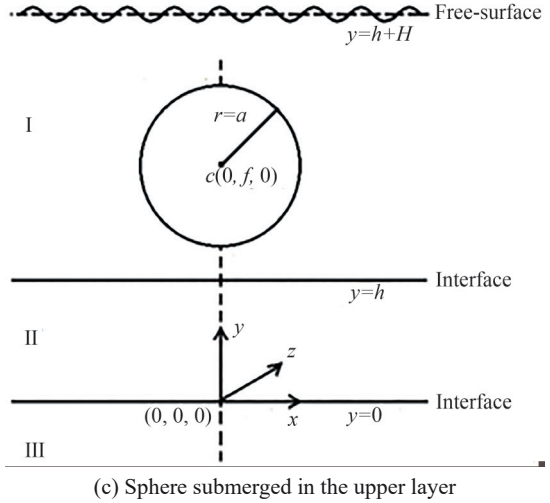

(c) Sphere submerged in the upper layer

Figure 1 Schematic diagrams of a sphere submerged in either layer of the three-layer fluid

3 Scattering by a submerged sphere

The centre of the sphere of radius a is taken as $(0, f, 0)$ so that for $f < 0$ and $a > f$, the sphere is in the lower layer and for $f > 0$ and $a < \min(h - f, f)$, $f < h$, the sphere is in the middle layer and $f > 0$ and $a < \min(H + h - f, f)$, $h < f < h + H$, the sphere is in the upper layer. Polar co-ordinates (r, θ, α) are defined by

$$x = r\sin\theta\cos\alpha,\ y = f - r\cos\theta, z = r\sin\theta\sin\alpha \quad (10)$$

so that $r = a$ denotes the surface of the sphere.

3.1 Sphere in the lower layer

A solution of Laplace's equation in the spherical polar co-ordinate system (r, θ, α) and singular at $r = 0$ is $r^{-n-1}P_n^m(\cos\theta)\cos m\alpha$, $n \geqslant m \geqslant 0$, where P_n^m are associated Legendre functions. This has the integral representation, valid for $y > f$

$$\frac{P_n^m(\cos\theta)}{r^{n+1}}\cos m\alpha = \frac{\cos m\alpha}{(n-m)!}\int_0^\infty k^n e^{-k(y-f)}J_m(kR)\,\mathrm{d}k \quad (11)$$

where J_m are Bessel functions and $R = (x^2 + z^2)^{1/2}$. Let the multipole potentials $\phi_n^{jm}\cos m\alpha$, j = I, II, III, $m = 0, 1$ be the singular solutions of the Laplace's equation and satisfy (2)−(6) and behave as outgoing waves as $R \to \infty$ which is the radiation condition. The multipole potentials $\phi_n^{\mathrm{I}m}$, $\phi_n^{\mathrm{II}m}$, $\phi_n^{\mathrm{III}m}$ are obtained as (cf. Das and Sahu 2021)

$$\phi_n^{\mathrm{I}m} = \frac{a^{n+1}}{(n-m)!}\int_0^\infty k^n\left(A(k)e^{ky} + B(k)e^{-ky}\right)J_m(kR)\,\mathrm{d}k \quad (12)$$

$$\phi_n^{\mathrm{II}m} = \frac{a^{n+1}}{(n-m)!}\int_0^\infty k^n\left(C(k)e^{ky} + D(k)e^{-ky}\right)J_m(kR)\,\mathrm{d}k \quad (13)$$

$$\phi_n^{\mathrm{III}m} = \left(\frac{a}{r}\right)^{n+1}P_n^m(\cos\theta) + \frac{a^{n+1}}{(n-m)!}\int_0^\infty k^n E(k)e^{ky}J_m(kR)\,\mathrm{d}k \quad (14)$$

where

$$A(k) = 4\frac{(k+K)K^2e^{kf}e^{-2k(h+H)}}{(1-s_1)(1-s_2)H(k)} \quad (15)$$

$$B(k) = 4\frac{K^2e^{kf}}{(1-s_1)(1-s_2)h(k)} \quad (16)$$

$$C(k) = 2\frac{K(k+K)e^{kf}\{(k+K\sigma_1)e^{-2k(h+H)} - (k-K)e^{-2kh}\}}{(1-s_2)H(k)} \quad (17)$$

$$D(k) = 2\frac{Ke^{kf}\left\{(k+K)e^{-2kH} - \left(k - K\sigma_1\right)\right\}}{\left(1 - s_2\right)h(k)} \tag{18}$$

$$E(k) = e^{kf}[\left(k + K\sigma_2\right)\left\{\left(k + K\sigma_1\right)e^{-2k(h+H)} - (k-K)e^{-2kh}\right\} - (k-K)\left\{(k+K)e^{-2kH} - (k - K\sigma_1)\right\}]\frac{k+K}{H(k)} \tag{19}$$

where $\sigma_1 = \frac{1+s_1}{1-s_1}$, $\sigma_2 = \frac{1+s_2}{1-s_2}$

and

$$H(k) = (k-K)h(k), \tag{20}$$

$$h(k) = (k+K)\left\{\left(k + K\sigma_1\right)e^{-2kH} - (k-K)\right\}e^{-2kh} - \left(k - K\sigma_2\right)\left\{(k+K)e^{-2kH} - (k - K\sigma_1)\right\} \tag{21}$$

Since the equation $H(k) = 0$ has exactly three positive real roots $K, k_1$and k_2 $(k_2 > k_1)$ (say), the path of integration is indented to pass beneath the poles of the above three integrands at $k = K$, $k = k_1$ and $k = k_2$.

The far-field forms of the multipoles, in the lower layer, is given by (cf. Das and Sahu 2021)

$$\phi_n^{\mathrm{III}m} \sim \frac{(-i)^{m+1}a^{n+1}}{(n-m)!}\left(\frac{2\pi}{R}\right)^{\frac{1}{2}}\left(K^{n-\frac{1}{2}}E^K e^{iKR+Ky} + k_1^{n-\frac{1}{2}}E^{k_1}e^{ik_1R+k_1y} + k_2^{n-\frac{1}{2}}E^{k_2}e^{ik_2R+k_2y}\right)e^{-i\frac{\pi}{4}} \tag{22}$$

as $R \to \infty$. Here E^K, E^{k_1} and E^{k_2} are the residues of $E(k)$ at $k = K$, $k = k_1$ and $k = k_2$ respectively, given by

$$E^K = 2K^3\frac{\left(1+\sigma_1\right)(1+\sigma_2)e^{Kf}e^{-2K(h+H)}}{h(K)} \tag{23}$$

$$E^{k_j} = e^{k_j f}[\left(k_j + K\sigma_2\right)\left\{\left(k_j + K\sigma_1\right)e^{-2k_j(h+H)} - \left(k_j - K\right)e^{-2k_j h}\right\} - \left(k_j - K\right)\left\{\left(k_j + K\right)e^{-2k_j H} - \left(k_j - K\sigma_1\right)\right\}]\frac{(k_j+K)}{H'\left(k_j\right)},\ j = 1,2 \tag{24}$$

Using the result

$$e^{\pm k(y-f)}J_m(kR) = (\pm 1)^m\sum_{q=m}^{\infty}\frac{(\pm kr)^q}{(q+m)!}P_q^m(\cos\theta) \tag{25}$$

(14) can be expressed as

$$\phi_n^{\mathrm{III}m} = \left(\frac{a}{r}\right)^{n+1}P_n^m(\cos\theta) + \sum_{s=m}^{\infty}A_{ns}^m r^s P_s^m(\cos\theta) \tag{26}$$

where

$$A_{ns}^m = \frac{a^{n+1}}{(n-m)!(s+m)!}\oint_0^{\infty}k^{n+s}E(k)e^{kf}\mathrm{d}k \tag{27}$$

3.1.1 Incident wave train of wavenumber *K*

First we consider an incident plane wave of wave number K and amplitude A on the free surface $y = h + H$ whose potential can be expanded in spherical plolar co-ordinates and get

$$\phi_{\mathrm{inc}} = -\frac{igA}{\omega}e^{K(y-h-H)}e^{iKR\cos\alpha}$$

$$= -\frac{igA}{\omega}e^{K(f-h-K)}\sum_{m=0}^{\infty}\epsilon_m i^m\cos m\alpha \tag{28}$$

$$\sum_{s=m}^{\infty}\frac{(Kr)^s}{(s+m)!}P_s^m(\cos\theta) \tag{29}$$

where $\epsilon_0 = 1, \epsilon_m = 2$ for $m \geqslant 1$.

For the scattering problems considered, we write

$$\phi_S = -\frac{igA}{\omega}\sum_{m=0}^{\infty}\sum_{n=m_1}^{\infty}c_n^m\phi_n^m\cos m\alpha \tag{30}$$

where $m_1 = \max(m,1)$ and ϕ_n^m is given (in the lower fluid layer) by (26).

If we then apply the boundary condition (9) and use the orthogonality of the associated Legendre functions and also the functions $\cos m\alpha$ we can derive an infinite system of equations for the sets of coefficients $c_n^m, n \geqslant m_1$ for each $m \geqslant 0$, which is

$$c_s^m - \frac{s}{s+1}\sum_{n=m_1}^{\infty}A_{ns}^m c_n^m = \frac{\epsilon_m i^m s(Ka)^s}{(\mathrm{s}+1)(\mathrm{s}+\mathrm{m})!}e^{K(f-h-H)},\quad s \geqslant m_1 \tag{31}$$

These system can be solved by truncation.

The hydrodynamic force on the body in the ith mode of motion can be written as $F_i(t) = \mathrm{Re}\{f_i e^{-i\omega t}\}$, where f_i is found by integrating the dynamic pressure times the appropriate component of the normal over the body surface. In other words,

$$f_i = i\rho_3\omega\int_{S_B}\phi n_i\,\mathrm{d}s$$

where S_B is the body boundary and n_i is the component of the inward normal to the body in the ith mode of motion.

The vertical and horizontal exciting forces on the sphere, $\bar{f}_K^0$ and $\bar{f}_K^1$ can be obtained as

$$\bar{f}_K^0 = -\frac{4}{3}\Pi a^2\rho_3 gA\left(Kae^{K(f-h-H)} + c_1^0 + \sum_{n=1}^{\infty}A_{n1}^0 c_n^0\right) \tag{32}$$

and

$$\bar{f}_K^1 = -\frac{4}{3}\Pi a^2 \rho_3 gA\left(iKae^{K(f-h-H)} + c_1^1 + \sum_{n=1}^{\infty} A_{n1}^1 c_n^1\right) \quad (33)$$

These can be simplified using (31) with $s = 1$ giving

$$\left|f_K^0\right| = \left|\frac{\bar{f}_K^0}{a^2\rho_3 gA}\right| = 4\pi\left|c_1^0\right| \quad (34)$$

and

$$\left|f_K^1\right| = \left|\frac{\bar{f}_K^1}{a^2\rho_3 gA}\right| = 4\pi\left|c_1^1\right| \quad (35)$$

The constants c_1^0 appearing in (34) and c_1^1 appearing in (35) can be obtained numerically by solving the linear system (31) after truncation.

3.1.2 Incident wave train of wavenumber k_j, j=1,2

Now, we consider the case of an incident plane wave of amplitude A on the interface $y = h$ for k_1 and $y = 0$ for k_2 and the wavenumber k_j described by

$$\phi_{\text{inc}}^{\text{III}} = -\frac{igAK}{\omega k_j} e^{k_j y + ik_j R\cos\alpha},\ j = 1, 2 \quad (36)$$

The analysis is very similar to that given above for an incident wave of wavenumber K. We use the same expansion for ϕ_S as before, Equation (30), but denote the unknown coefficients by d_n^m and we obtain the infinite system of equations

$$d_s^m - \frac{s}{s+1}\sum_{n=m_1}^{\infty} A_{ns}^m d_n^m = \frac{\epsilon_m i^m sKa\left(k_j a\right)^{s-1}}{(\mathrm{s}+1)(\mathrm{s}+\mathrm{m})!} e^{k_j f},$$
$$s \geqslant m_1,\ j = 1, 2 \quad (37)$$

for each $m \geqslant 0$.

The expressions for the vertical and horizontal exciting forces are

$$\left|f_{k_j}^0\right| = \left|\frac{\bar{f}_{k_j}^0}{a^2\rho_3 gA}\right| = 4\pi\left|d_1^0\right|,\ j = 1, 2 \quad (38)$$

and

$$\left|f_{k_j}^1\right| = \left|\frac{\bar{f}_{k_j}^1}{a^2\rho_3 gA}\right| = 4\pi\left|d_1^1\right|\ j = 1, 2 \quad (39)$$

The constants d_1^0 appearing in (38) and d_1^1 appearing in (39) can be obtained numerically by solving the linear system (37) after truncation.

3.1.3 Numerical results

To study the numerical results the density ratios s_1 and s_2 are both taken to be 0.95. Figures 2 to 7 depict the time-independent and non-dimensional vertical and horizontal exciting forces on the sphere submerged in the lower layer, plotted against the wavenumber Ka for the incident wave of wavenumbers K, k_1 and k_2.We have chosen h/a and H/a as 2, when the sphere is submerged in the lower layer for various immersion depths $f/a = -1.1, -1.5, -2$ and -3, shown using four distinct curves. $f/a = -1.1$ represents the immersion depth of the sphere almost close to the interface $y = 0$, between the lower and the middle layer. The curves corresponding to other values of f/a represent the sphere submerged deeper below the interface. It is noted that the forces in all of these figures increase with the increase in Ka and attain a maximum after which they decrease with further increase in Ka. Naturally, the forces increase as the submersion depth of the sphere decreases when the surface of the sphere comes nearer to the interface $y = 0$ ($f/a = -1.1$) and consequently, to the free surface. The forces have similar behaviour as those of Cadby and Linton (2000), when the sphere is submerged in the lower layer, though here, in three-layer fluid the forces are higher and even the increase in forces becomes larger with the increase in submersion depths. Again, the range of forces is more here than that of Cadby and Linton (2000), where the fluid was considered of two layers.

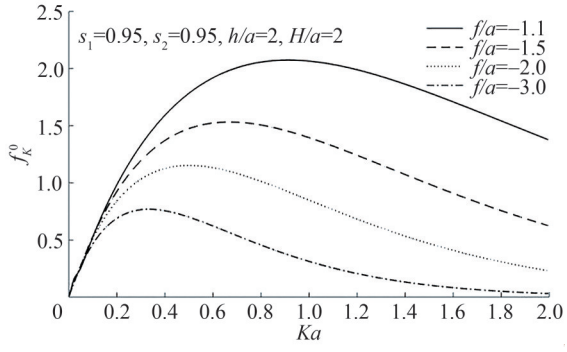

Figure 2 Vertical forces f_K^0 plotted against Ka in lower layer

Also, the Tables 1 and 2 corresponding to heaving and swaying spheres show the values of vertical and horizontal forces in the two-layer fluid (paper of Cadby and Linton (2000)) and the present paper of three-layer fluid. For all data we consider $s_1 = 0.99$, depth of the upper layer in two-layer fluid being 4, $h/a = 2$ and $H/a = 2$ in three layer fluid and $f/a = -2$ for both the cases. Thus it may be noted that for $s_1 = 0.99$, the density ratio of the upper and middle layer, then the density of the upper and middle layer are almost same and we see that the three-layer fluid becomes two-layer fluid. For this case it is observed that from the Tables 1 and 2 the values of the vertical and hori-

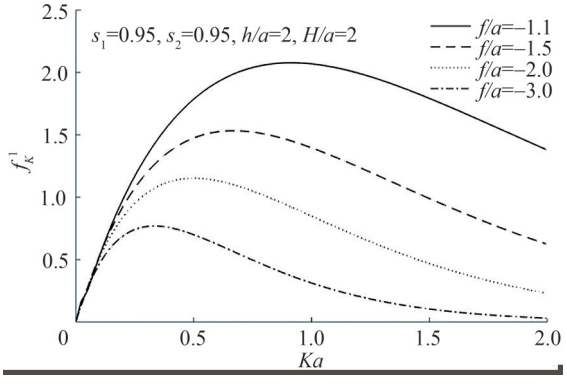

Figure 3 Horizontal forces f_K^1 plotted against Ka in lower layer

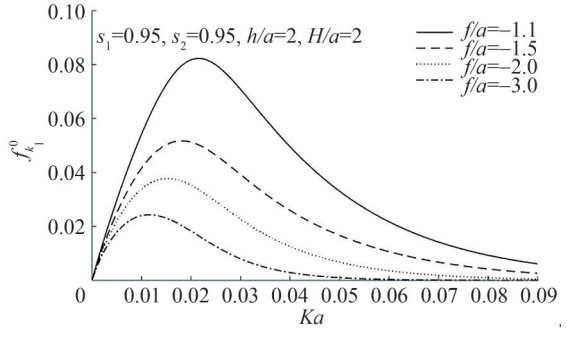

Figure 4 Vertical forces $f_{k_1}^0$ plotted against Ka in lower layer

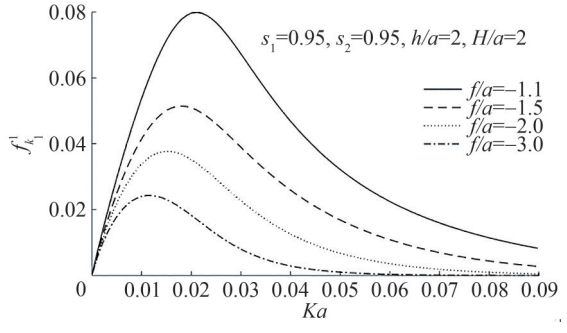

Figure 5 Horizontal forces $f_{k_1}^1$ plotted against Ka in lower layer

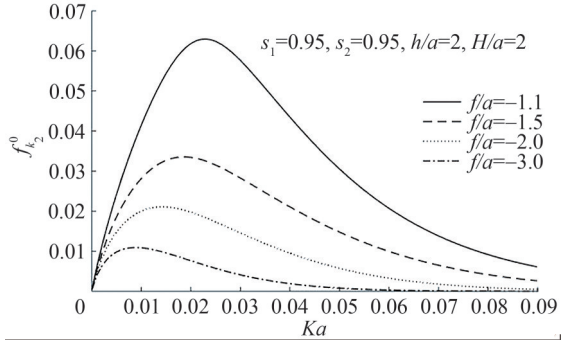

Figure 6 Vertical forces $f_{k_2}^0$ plotted against Ka in lower layer

zontal forces almost coincide with the corresponding values for a two-layer fluid.

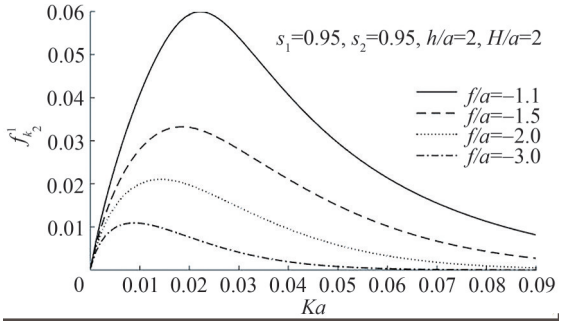

Figure 7 Horizontal forces $f_{k_2}^1$ plotted against Ka in lower layer

Table 1 Vertical exciting forces for the sphere in lower layer fluid

Ka	Case of two-layer fluid (Cadby and Linton 2000)	Case of three layer fluid
0.2	0.377 856	0.377 845
0.4	0.227 311	0.227 306
0.6	0.102 709	0.102 707
0.8	0.041 266 4	0.041 265 6
1.0	0.015 541 1	0.015 540 9
1.2	0.005 617 94	0.005 617 85
1.4	0.001 974 26	0.001 974 23
1.6	0.000 679 608	0.000 679 598
1.8	0.000 230 284	0.000 230 28
2.0	0.000 077 066 6	0.000 077 065 4

Table 2 Horizontal exciting forces for the sphere in lower layer fluid

Ka	Case of two-layer fluid (Cadby and Linton 2000)	Case of three layer fluid
0.2	0.377 871	0.377 861
0.4	0.227 327	0.227 321
0.6	0.102 719	0.102 717
0.8	0.041 271 2	0.041 270 4
1.0	0.015 543 1	0.015 542 8
1.2	0.005 618 72	0.005 618 63
1.4	0.001 974 56	0.001 974 53
1.6	0.000 679 723	0.000 679 713
1.8	0.000 230 327	0.000 230 323
2.0	0.000 077 082 4	0.000 077 081 3

The vertical and horizontal exciting forces for an incident wave of wavenumber K are shown in Figures 2 and 3. They are very similar. Figures 4 and 5 depict the vertical and horizontal exciting forces respectively, for the incident wave of wavenumber k_1 and Figures 6 and 7, depict the same respectively, for the incident wave of wavenumber k_2, where in both the cases, vertical exciting forces are slightly greater than horizontal exciting forces. For Figures 4 and 5, the forces are much smaller than those of Figures 2 and 3, and the forces of Figures 6 and 7 are smaller than those of the previous figures.

3.2 Sphere in the middle layer

For the problem involving a sphere in the middle layer, one needs to construct the multipoles which are singular at $y = f > 0$. Suitable multipoles are obtained as (cf. Das and Sahu 2021)

$$\phi_n^{\mathrm{I}m} = \frac{(-1)^{m+n}a^{n+1}}{(n-m)!}\oint_0^\infty k^n (A_M(k)e^{ky} + B_M(k)e^{-ky})J_m(kR)\,\mathrm{d}k \tag{40}$$

$$\phi_n^{\mathrm{II}m} = \left(\frac{a}{r}\right)^{n+1} P_n^m(\cos\theta) + \frac{(-1)^{m+n}a^{n+1}}{(n-m)!} \oint_0^\infty k^n (C_M(k)e^{ky} + D_M(k)e^{-ky})J_m(kR)\,\mathrm{d}k \tag{41}$$

$$\phi_n^{\mathrm{III}m} = \frac{(-1)^{m+n}a^{n+1}}{(n-m)!}\oint_0^\infty k^n E_M(k)e^{ky}J_m(kR)\,\mathrm{d}k \tag{42}$$

where

$$A_M(k) = 2\frac{(k+K)Ke^{-2k(h+H)}}{(1-s_1)H(k)}\begin{bmatrix}(-1)^{n+m}(K\sigma_2 - k)e^{kf}\\ -(k-K)e^{-kf}\end{bmatrix} \tag{43}$$

$$B_M(k) = 2\frac{K}{(1-s_1)h(k)}\begin{bmatrix}(-1)^{n+m}(K\sigma_2 - k)e^{kf}\\ -(k-K)e^{-kf}\end{bmatrix} \tag{44}$$

$$C_M(k) = \frac{(k-K)e^{-2kh} - (k+K\sigma_1)e^{-2k(h+H)}}{H(k)} \times\left[(k+K)\left\{(k-K)e^{-kf} - (-1)^{n+m}(K\sigma_2 - k)e^{kf}\right\}\right] \tag{45}$$

$$D_M(k) = \frac{(-1)^{n+m}(k+K)e^{kf}\left\{(k-K)e^{-2kh} - (k+K\sigma_1)e^{-2k(h+H)}\right\}}{h(k)} - \frac{(k-K)e^{-kf}\left\{(K\sigma_1 - k) + (k+K)e^{-2kH}\right\}}{h(k)} \tag{46}$$

$$E_M(k) = e^{-kf} + C_M(k) - D_M(k) \tag{47}$$

and the path of integration is indented to pass beneath the poles of the above three integrands at $k = K, k = k_1$ and $k = k_2$.

The polar expansions of the multipoles, similar to the case when sphere is in the lower fluid, are

$$\phi_n^{\mathrm{II}m} = \left(\frac{a}{r}\right)^{n+1} P_n^m(\cos\theta) + \sum_{s=m}^\infty B_{ns}^m r^s P_s^m(\cos\theta) \tag{48}$$

where

$$B_{ns}^m = \frac{(-1)^{m+n}a^{n+1}}{(n-m)!(s+m)!}\oint_0^\infty k^{n+s}(C_M(k)e^{kf} + (-1)^{m+s}D_M(k)e^{-kf})\,\mathrm{d}k \tag{49}$$

3.2.1 Incident wave train of wavenumber *K*

An incident wave of wavenumber K on the free surface has the same form in the middle layer as in the lower layer given by (28). The total Potential ϕ_S can be expanded using (30), but it now uses the multipole expansions developed for the middle layer, (48). Thus the coefficients c_n^m satisfy the infinite system of equations

$$c_s^m - \frac{s}{s+1}\sum_{n=m_1}^\infty B_{ns}^m c_n^m = \frac{\epsilon_m i^m s(Ka)^s}{(s+1)(s+m)!}e^{K(f-h-H)}, \quad s \geqslant m_1 \tag{50}$$

and the non-dimensional vertical and horizontal forces for a sphere in the middle layer fluid through the equations

$$\left|f_K^0\right| = \left|\frac{\bar{f}_K^0}{a^2\rho_2 gA}\right| = 4\pi\left|c_1^0\right| \tag{51}$$

and

$$\left|f_K^1\right| = \left|\frac{\bar{f}_K^1}{a^2\rho_2 gA}\right| = 4\pi\left|c_1^1\right| \tag{52}$$

3.2.2 Incident wave train of wavenumber k_j, j=1,2

For this problem $\phi_{\mathrm{inc}}^{\mathrm{II}}$ is given, in the middle fluid, by $-\frac{igAK}{\omega k_j}g_2^j(y)e^{ik_j\cos\alpha}$, $j = 1, 2$, where

$$g_2^j(y) = \frac{(k_j - K\sigma_2)e^{k_j y} + (k_j - K)e^{-k_j y}}{K(1-\sigma_2)}, \quad j = 1, 2 \tag{53}$$

The polar expansion of $\phi_{\mathrm{inc}}^{\mathrm{II}}$ is given by

$$\phi_{\mathrm{inc}}^{\mathrm{II}} = -\frac{igA}{\omega}\sum_{m=0}^\infty \epsilon_m i^m \cos m\alpha \sum_{s=m}^\infty \frac{(k_j r)^s}{(s+m)!}M_1(k_j)P_s^m(\cos\theta), \quad j = 1,2 \tag{54}$$

where $\epsilon_0 = 1$, $\epsilon_m = 2$ for $m \geqslant 1$, where

$$M_1(k_j) = 2\frac{(k_j - K\sigma_2)e^{k_j(f-h)} + (-1)^{m+s}(k_j - K)e^{-k_j(f+h)}}{k_j(1-\sigma_2)}, \quad j = 1, 2$$

For each $m \geqslant 0$ the coefficients d_n^m, in the expansion ϕ_{S} satisfy the infinite system of equations

$$d_s^m - \frac{s}{s+1}\sum_{n=m_1}^{\infty} B_{ns}^m d_n^m = \frac{\epsilon_m i^m s\left(k_j a\right)^s}{(s+1)(s+m)!} M_1\left(k_j\right),\ s \geqslant m_1,$$

$$j = 1, 2 \tag{55}$$

for each $m \geqslant 0$.

Also, the expressions for the non-dimensional vertical and horizontal exciting forces are

$$\left| f_{k_j}^0 \right| = \left| \frac{\bar{f}_{k_j}^0}{a^2 \rho_2 g A} \right| = 4\pi \left| d_1^0 \right|,\ j = 1,2 \tag{56}$$

and

$$\left| f_{k_j}^1 \right| = \left| \frac{\bar{f}_{k_j}^1}{a^2 \rho_2 g A} \right| = 4\pi \left| d_1^1 \right|\ j = 1,2 \tag{57}$$

The constants d_1^0 appearing in (56) and d_1^1 appearing in (57) can be obtained numerically by solving the linear system (55) after truncation. Here the linear system (55) is truncated up to five terms. This provides an accuracy up to five decimal places, because if the system is truncated up to five or six terms, there is practically no change in the numerical results.

3.2.3 Numerical results

When the sphere is submerged in the middle layer, the vertical and horizontal exciting forces are represented with four curves corresponding to the various submersion depths of the sphere f/a = 1.1, 1.7, 2.3 and 2.9 and the density ratios s_1, s_2 are both taken to be 0.95. Here we have chosen, h/a and H/a both as 4. In all the figures, the forces are higher when the surface of the sphere is closer to either interface $y = 0$ or $= h$ (f/a = 1.1, 2.9). Figures 8 and 9 portray that the vertical and horizontal exciting forces associated with the incident wave of wavenumber K are of similar characteristics. Figures 10 and 11 depict the vertical and horizontal exciting forces respectively, for the incident wave of wavenumber k_1. The maximum of vertical exciting forces occurs at higher values of Ka than that of horizontal exciting forces. Again, in this case, the maximums for vertical exciting forces are higher than those of horizontal exciting forces. This same nature is also noted for the vertical and horizontal exciting forces associated with the incident wave of wavenumber k_2, as shown in Figures 12 and 13.

For the sphere submerged in the middle layer, all the forces increase with the increase in Ka, and after attaining the maximum, they decrease with further increase in Ka, but only some horizontal forces corresponding to particular submersion depths of the sphere, associated with the incident wave of wavenumber k_1, become zero which again increase and after reaching a local maximum, they decrease as Ka further increases. The forces for the sphere near to the interface $y = 0$, between the lower and middle

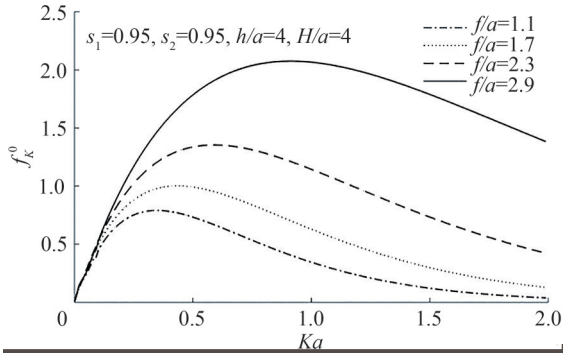

Figure 8 Vertical forces f_K^0 plotted against Ka in middle layer

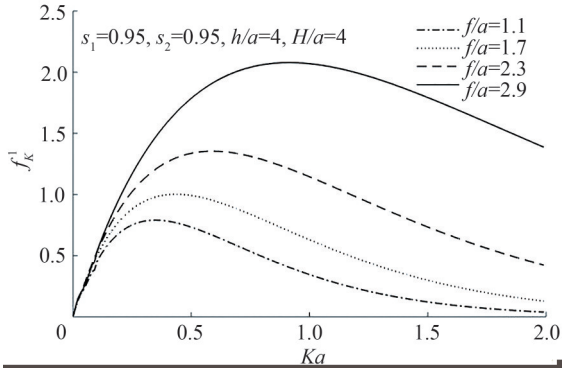

Figure 9 Horizontal forces f_K^1 plotted against Ka in middle layer

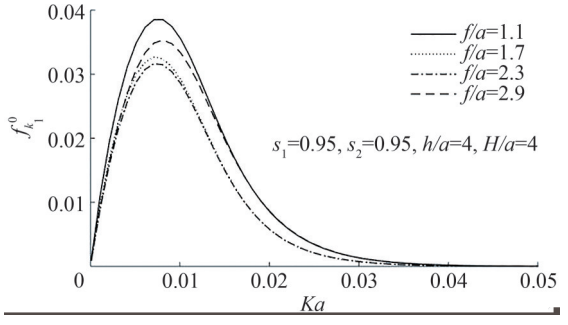

Figure 10 Vertical forces $f_{k_1}^0$ plotted against Ka in middle layer

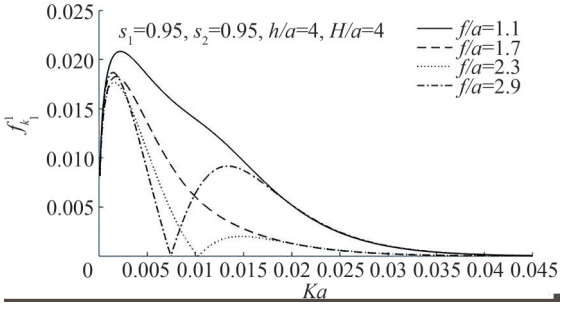

Figure 11 Horizontal forces $f_{k_1}^1$ plotted against Ka in middle layer

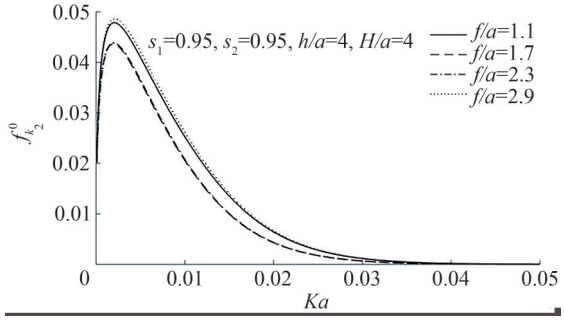

Figure 12 Vertical forces $f^0_{k_2}$ plotted against Ka in middle layer

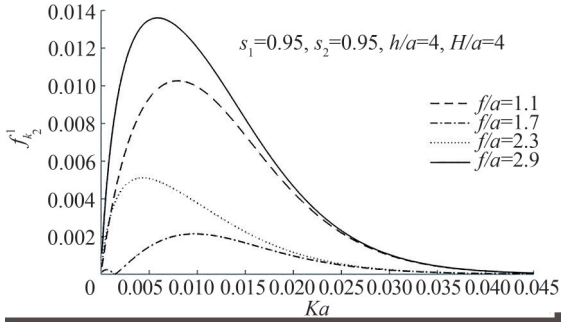

Figure 13 Horizontal forces $f^1_{k_2}$ plotted against Ka in middle layer

layer (f/a = 1.1), is the highest for the incident wave of wavenumber k_1 (Figures 10, 11), whereas those for the sphere near to the interface $y = h$, between the upper and the middle layer (f/a = 2.9), is the highest for the incident wave of wavenumber k_2 (Figures 12, 13) as it is associated with this interface. From Figures 12 and 13, we also observe that for the incident wave of wavenumber k_2, the maximum of vertical and horizontal exciting forces occurs for larger waves (smaller wavenumbers) compared to those for the incident wave of wavenumber K (Figures 8, 9), but compared to those for the incident wave of wavenumber k_1 (Figures 10, 11), the maximum of vertical exciting forces for the incident wave of wavenumber k_2 occur for slightly smaller values of Ka and those for horizontal exciting forces occur for slightly larger values of Ka.

Also, the tables 3 and 4 corresponding to heaving and swaying spheres show the values of vertical and horizontal forces in the two-layer fluid (paper of Cadby and Linton 2000) and the present paper of three-layer fluid. For all data we consider s_1 = 0.99, depth of the upper layer in two-layer fluid being 6, h/a = 3 and H/a = 3 in three-layer fluid and f/a = 1.7 for both the cases. Thus, it may be noted that for s_1 = 0.99, the density ratio of the upper and middle layer, then the density of the upper and the middle layer are almost same and we see that the three-layer fluid becomes two-layer fluid. For this case it is observed that from the tables 3 and 4 the values of the vertical and horizontal forces almost coincide with the corresponding values for a two-layer fluid.

Table 3 Vertical exciting forces for the sphere in middle layer fluid

Ka	Case of two-layer fluid (Cadby and Linton 2000)	Case of three layer fluid
0.2	0.516 574	0.516 515
0.4	0.448 846	0.448 833
0.6	0.284 237	0.284 214
0.8	0.160 359	0.160 393
1.0	0.084 881 5	0.084 887 9
1.2	0.043 130 5	0.043 138 7
1.4	0.021 302 5	0.021 301 8
1.6	0.010 305 0	0.010 304 8
1.8	0.004 906 59	0.004 906 59
2.0	0.002 307 21	0.002 307 77

Table 4 Horizontal exciting forces for the sphere in middle layer fluid

Ka	Case of two layer fluid (Cadby and Linton 2000)	Case of three layer fluid
0.2	0.515 021	0.515 032
0.4	0.448 747	0.448 795
0.6	0.284 252	0.284 233
0.8	0.160 384	0.160 384
1.0	0.084 899 4	0.084 890 5
1.2	0.043 140 5	0.043 142
1.4	0.021 307 7	0.021 309 1
1.6	0.010 307 7	0.010 308 7
1.8	0.004 907 93	0.004 907 64
2.0	0.002 307 88	0.002 307 84

3.3 Sphere in the upper layer

For the problem involving a sphere in the upper layer, one needs to construct the multipoles which are singular at $y = f > 0$. Suitable multipoles are obtained as (cf. Das and Sahu 2021)

$$\phi_n^{\mathrm{I}m} = \left(\frac{a}{r}\right)^{n+1} P_n^m(\cos\theta) + \frac{(-1)^{m+n}a^{n+1}}{(n-m)!}\oint_0^\infty k^n (A_U(k)e^{ky} + B_U(k)e^{-ky})J_m(kR)\,\mathrm{d}k \tag{58}$$

$$\phi_n^{\mathrm{II}m} = \frac{(-1)^{m+n}a^{n+1}}{(n-m)!}\oint_0^\infty k^n (C_U(k)e^{ky} + D_U(k)e^{-ky})J_m(kR)\,\mathrm{d}k \tag{59}$$

$$\phi_n^{\mathrm{III}m} = \frac{(-1)^{m+n}a^{n+1}}{(n-m)!}\oint_0^\infty k^n E_U(k)e^{ky}J_m(kR)\,\mathrm{d}k \tag{60}$$

where

$$A_U(k) = \frac{(k+K)(k-K)e^{-kf}e^{-2kH}\left\{-\left(k+K\sigma_1\right)e^{-2kh}+\left(k-K\sigma_2\right)\right\}}{H(k)} + (-1)^{n+m}(k+K)e^{-2k(h+H)}e^{kf} \times \frac{(k-K\sigma_1)(k-K\sigma_2)-(k+K)(k-K)e^{-2kh}}{H(k)} \quad (61)$$

$$B_U(k) = \left[(-1)^{n+m}(k+K)e^{-2kH}e^{kf} + (k-K)e^{-kf+2kh}\right]\frac{\left(k-K\sigma_2\right)-\left(k+K\sigma_1\right)e^{-2kh}}{h(k)} \quad (62)$$

$$C_U(k) = -2Ks_1(k-K\sigma_2)\frac{(-1)^{n+m}(k+K)e^{-2k(h+H)}e^{kf}+(k-K)e^{-kf}}{(1-s_1)H(k)} \quad (63)$$

$$D_U(k) = -2Ks_1\frac{(-1)^{n+m}(k+K)e^{-2k(h+H)}e^{kf}+(k-K)e^{-kf}}{(1-s_1)h(k)} \quad (64)$$

$$E_U(k) = C_U(k) - D_U(k) \quad (65)$$

and the path of integration is indented to pass beneath the poles of the above three integrands at $k = K$, $k = k_1$ and $k = k_2$.

The polar expansions of the multipoles, similar to the case when sphere is in the lower fluid, are

$$\phi_n^{\mathrm{Im}} = \left(\frac{a}{r}\right)^{n+1} P_n^m(\cos\theta) + \sum_{s=m}^{\infty} C_{ns}^m r^s P_s^m(\cos\theta) \quad (66)$$

where

$$C_{ns}^m = \frac{(-1)^{m+n}a^{n+1}}{(n-m)!(s+m)!}\int_0^{\infty} k^{n+s}\left(A_U(k)e^{kf} + (-1)^{m+s}B_U(k)e^{-kf}\right)\mathrm{d}k \quad (67)$$

3.3.1 Incident wave train of wavenumber *K*

An incident wave of wavenumber K on the free surface has the same form in the upper layer as in the lower layer given by (28). The total Potential ϕ_S can be expanded using (30), but it now uses the multipole expansions developed for the upper layer, (66). Thus the coefficients c_n^m satisfy the infinite system of equations

$$c_s^m - \frac{s}{s+1}\sum_{n=m_1}^{\infty} C_{ns}^m c_n^m = \frac{\epsilon_m i^m s(Ka)^s}{(s+1)(s+m)!}e^{K(f-h-H)}, \quad s \geqslant m_1 \quad (68)$$

and the non-dimensional vertical and horizontal forces for a sphere in the upper layer fluid through the equations

$$\left|f_K^0\right| = \left|\frac{\bar{f}_K^0}{a^2\rho_1 gA}\right| = 4\pi\left|c_1^0\right| \quad (69)$$

and

$$\left|f_K^1\right| = \left|\frac{\bar{f}_K^1}{a^2\rho_1 gA}\right| = 4\pi\left|c_1^1\right| \quad (70)$$

3.3.2 Incident wave train of wavenumber k_j, j=1,2

For this problem ϕ_{inc}^I is given, in the upper fluid, by $-\frac{igAK}{\omega k_j}g_1^j(y)e^{ik_j\cos\alpha}$, $j = 1, 2$ where

$$g_1^j(y) = 2\frac{\left(k_j+K\right)e^{-k_j(2h+2H-y)}+\left(k_j-K\right)e^{-k_j y}}{\left(1-s_1\right)\left(1-\sigma_2\right)\left\{\left(k_j+K\right)e^{-2k_jH}-\left(k_j-K\sigma_1\right)\right\}}, \quad j = 1, 2 \quad (71)$$

The polar expansion of $\phi_{\mathrm{inc}}^{\mathrm{I}}$ is given by

$$\phi_{\mathrm{inc}}^{\mathrm{I}} = -\frac{igA}{\omega}\sum_{m=0}^{\infty}\epsilon_m i^m\cos m\alpha\sum_{s=m}^{\infty}\frac{\left(k_j r\right)^s}{(s+m)!}M_2\left(k_j\right)P_s^m(\cos\theta), \quad j = 1, 2 \quad (72)$$

where $\epsilon_0 = 1$, $\epsilon_m = 2$ for $m \geqslant 1$, where

$$M_2(k_j) = 2\frac{\left(k_j+K\right)e^{-k_j(-f+2h+2H)}+(-1)^{m+s}(k_j-K)e^{-k_j(f+h+H)}}{(1-s_1)(1-\sigma_2)\left\{\left(k_j+K\right)e^{-2k_jH}-\left(k_j-K\sigma_1\right)\right\}}, \quad j = 1, 2$$

For each $m \geqslant 0$ the coefficients d_n^m, in the expansion ϕ_{S} satisfy the infinite system of equations

$$d_s^m - \frac{s}{s+1}\sum_{n=m_1}^{\infty} C_{ns}^m d_n^m = \frac{\epsilon_m i^m s\left(k_j a\right)^s}{(s+1)(s+m)!}M_2\left(k_j\right), \; s \geqslant m_1, \quad j = 1, 2 \quad (73)$$

for each $m \geqslant 0$.

Also, the expressions for the non-dimensional vertical and horizontal exciting forces are

$$\left|f_{k_j}^0\right| = \left|\frac{\bar{f}_{k_j}^0}{a^2\rho_1 gA}\right| = 4\pi\left|d_1^0\right|, \; j = 1, 2 \quad (74)$$

and

$$\left| f_{k_j}^1 \right| = \left| \frac{\bar{f}_{k_j}^1}{a^2 \rho_1 g A} \right| = 4\pi \left| d_1^1 \right| \; j = 1,2 \qquad (75)$$

The constants d_1^0 appearing in (74) and d_1^1 appearing in (75) can be obtained numerically by solving the linear system (73) after truncation. Here the linear system (73) is truncated up to five terms. This provides an accuracy up to five decimal places, because if the system is truncated up to five or six terms, there is practically no change in the numerical results.

3.3.3 Numerical results

The vertical and horizontal exciting forces on the sphere submerged in the upper layer of the three-layer fluid with the submersion depths f/a = 5.1, 5.7, 6 and 6.8, are depicted by four curves for each f/a. To analyze this case also, we have chosen h/a and H/a both as 4. It is observed that the maximum for vertical and horizontal exciting forces are similar for an incident wave of a particular wavenumber.

The vertical and horizontal exciting forces for the incident wave of wavenumber K, k_1 and k_2 are shown by Figures 14, 15; 16, 17; and 18, 19 respectively. For the incident wave of wavenumber K, the forces are higher when the sphere is near to the free surface (f/a = 6.8). However, for the incident waves of wavenumbers k_1 and k_2, the forces increase with the decrease in f/a. Hence, the forces are high when the surface of the submerged sphere comes closer to the interface $y = h$ (f/a = 5.1). Both the vertical and horizontal exciting forces are higher for the incident wave of wavenumber K (Figures 14, 15) than those for the

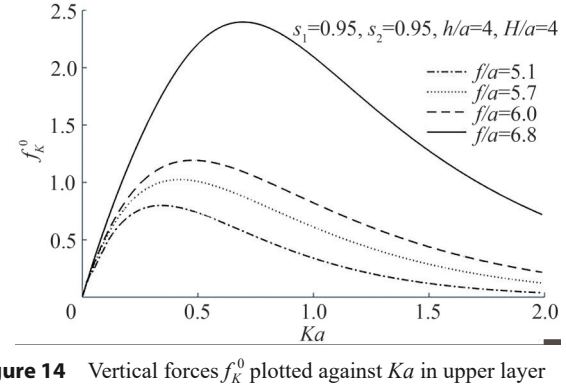

Figure 14 Vertical forces f_K^0 plotted against Ka in upper layer

incident wave of wavenumbers k_1 (Figures 16, 17) and k_2 (Figures 18, 19). For the incident wave of wavenumbers k_1 and k_2, the vertical exciting forces may attain the maximum at a slightly smaller value of Ka than those of horizontal exciting forces.

Also, the Tables 5 and 6 corresponding to heaving and swaying spheres show the values of vertical and horizontal forces in the two-layer fluid (paper of Cadby and Linton 2000) and the present paper of three-layer fluid. For all data we consider s_1 = 0.99, depth of the upper layer in two-layer fluid being 6, h/a = 3 and H/a = 3 in three-layer fluid and f/a = 5.7 for both the cases. Thus, it may be noted

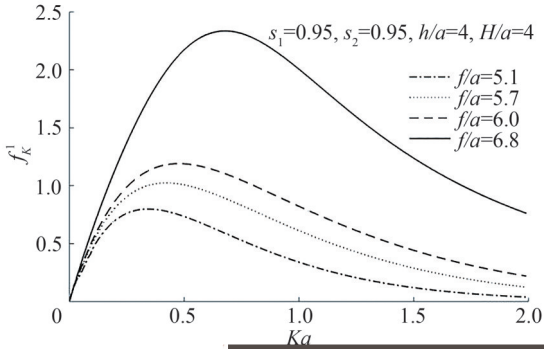

Figure 15 Horizontal forces f_K^1 plotted against Ka in upper layer

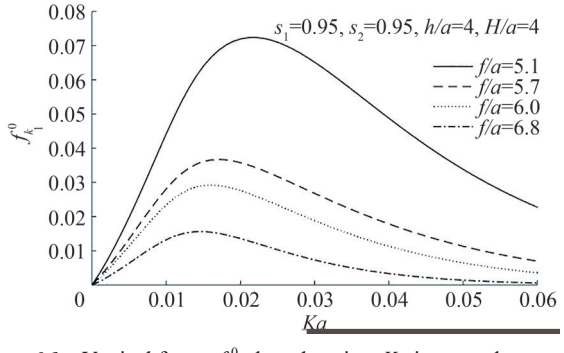

Figure 16 Vertical forces $f_{k_1}^0$ plotted against Ka in upper layer

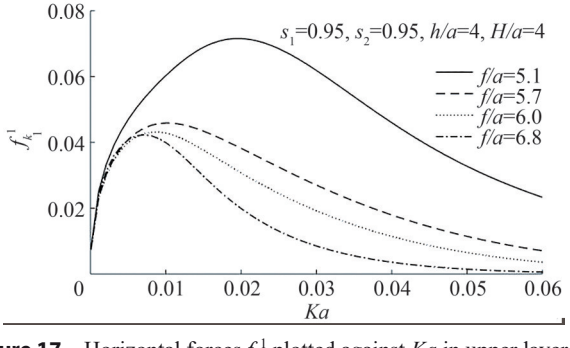

Figure 17 Horizontal forces $f_{k_1}^1$ plotted against Ka in upper layer

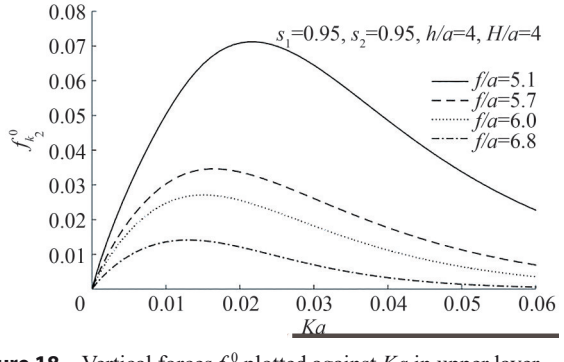

Figure 18 Vertical forces $f_{k_2}^0$ plotted against Ka in upper layer

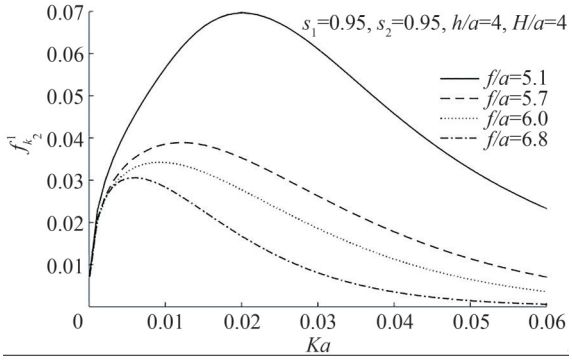

Figure 19 Horizontal forces $f^1_{k_2}$ plotted against Ka in upper layer

that for s_1 = 0.99, the density ratio of the upper and middle layer, then the density of the upper and the middle layer are almost same and we see that the three-layer fluid becomes two-layer fluid. For this case it is observed that from the Tables 5 and 6 the values of the vertical and horizontal forces almost coincide with the corresponding values for a two-layer fluid.

Table 5 Vertical exciting forces for the sphere in upper layer fluid

Ka	Case of two-layer fluid (Cadby and Linton 2000)	Case of three layer fluid
0.2	1.088 8	1.088 32
0.4	1.778 42	1.778 48
0.6	2.099 32	2.099 77
0.8	2.106 75	2.106 27
1.0	1.915 37	1.915 12
1.2	1.639 67	1.639 6
1.4	1.355 25	1.355 19
1.6	1.098 3	1.098 9
1.8	0.880 291	0.880 224
2.0	0.700 992	0.700 92

Table 6 Horizontal exciting forces for the sphere in upper layer fluid

Ka	Case of two-layer fluid (Cadby and Linton 2000)	Case of three layer fluid
0.2	1.086 18	1.086 69
0.4	1.765 24	1.765 33
0.6	2.068 26	2.068 29
0.8	2.059 91	2.059 46
1.0	1.864 32	1.864 54
1.2	1.597 75	1.597 64
1.4	1.331 42	1.331 02
1.6	1.095 67	1.095 42
1.8	0.897 506	0.897 557
2.0	0.734 207	0.734 202

In all three cases, it is noted that the maximum of the forces for the incident wave of wavenumbers k_1 and k_2, occur for larger waves (smaller wavenumbers) than those for the incident wave of wavenumber K. Thus, it is observed that when the densities of the upper and middle layer are taken as almost the same, that is when s_1 is almost equal to 1, the three-layer fluid behaves similar to two-layer fluid with free surface and both the vertical and horizontal exciting forces are somewhat similar to the vertical and horizontal exciting forces as represented by Cadby and Linton (2000) for two-layer fluid. Here due to the presence of more layer of the fluids, the curves for both vertical and horizontal forces are somewhat different from the curves for the same in the upper layer cases in the two-layer fluid given by Cadby and Linton (2000). They are oscillatory in nature. This may be attributed to interaction of the boundary of the sphere, free surface and interfaces between upper and middle layer as well as middle and lower layer.

4 Conclusion

We have examined the interaction between the incident waves with the sphere submerged in either layer of a three-layer fluid. The middle layer is of finite depth and is bounded above by an upper layer of finite depth with free surface and the lower layer extends infinitely downwards. In such a situation propagating waves can exist at three different wavenumbers for any given frequency. The method of multipoles expansion is used to solve the scattering problems for the sphere situated entirely within either of the layer of three-layer fluid. Numerical results for the vertical and horizontal forces for the sphere are obtained. The hydrodynamic forces are depicted graphically against the wavenumber as a number of figures when the sphere is submerged in either of the layers. When the density ratio of the upper and middle layer is made to approximately one, curves for vertical and horizontal forces almost coincide with the corresponding curves for the case of a two-layer fluid with a free surface. This means that in the limit, the density ratio of the upper and middle layer goes to approximately one, the solution agrees with the solution for the case of a two-layer fluid with a free surface.

References

Amran I, Isa K (2020) Modelling analysis of spherical underwater robot for aquaculture biofouling cleaning. Proceedings of the 12th National Technical Seminar on Unmanned System Technology, 29-45. DOI: 10.1007/978-981-16-2406-3_3

Cadby JR, Linton CM (2000) Three-dimensional water wave scattering in two-layers fluids. J Fluid Mech 423: 155-173. DOI: 10.1017/S0022112000002007

Chakrabarti A, Daripa P, Hamsapriye (2005) Trapped modes in a channel containing three layers of fluids and a submerged cylinder. Z Angew Math Phys 56(6): 1084-1097. DOI: 10.1007/s00033-005-5041-z

Chatjigeorgiou IK (2013) The analytic solution for hydrodynamic diffraction by submerged prolate spheroids in infinite water depth. J Eng Math 81(1): 47-65. DOI: 10.1007/s10665-012-9581-x

Chatjigeorgiou IK, Miloh T (2015) Rdiation and oblique diffraction by submerged prolate spheroids in water of finite depth. J Ocean Eng Mar Energy 1(1): 3-18. DOI: 10.1007/s40722-014-0001-3

Chatjigeorgiou IK, Miloh T (2017) Hydrodynamics of non-axisymmetric oblate spheroids below a free surface. J Ocean Eng Mar Energy 3(2): 125-138. DOI: 10.1007/s40722-017-0076-8

Chen MJ, Forbes LK (2008) Steady periodic waves in a three-layer fluid with shear in the middle layer. J Fluid Mech 594: 157-181. DOI: 10.1017/S0022112007008877

Das D (2008) Solution of the dispersion equation for internal waves in two-layer fluid with an ice-cover. Bull Cal Math Soc 100(2): 165-176

Das D (2015) Construction of wave-free potentials and multipoles in a two-layer fluid having free surface boundary condition with higher-order derivatives. J Mar Sci Appl 14(3): 270-282. DOI: 10.1007/s11804-015-1321-y

Das D (2016) Wave scattering by a horizontal circular cylinder in a three-layer fluid. J Ocean Engng Sci 1(2): 135-148. DOI: 10.1016/j.joes.2016.03.001

Das D, Majumder M (2020) Oblique waves scattering in three-layer fluid. Bull Cal Math Soc 112(2): 133-154

Das D, Mandal BN (2006) Oblique wave scattering by a circular cylinder in two-layer fluid with an ice-cover. 21st IWWWFB, 29-32

Das D, Mandal BN (2007) Wave scattering by a horizontal circular cylinder in a two-layer fluid with an ice-cover. International J Engng Sci 45(10): 842-872. DOI: 10.1016/j.ijengsci.2007.05.008

Das D, Mandal BN (2008) Water wave radiation by a sphere submerged in water with an ice-cover. Arch appl Mech 78(8): 649-661. DOI: 10.1007/s00419-007-0186-1

Das D, Mandal BN (2010) Wave radiation by a sphere submerged in a two-layer ocean with an ice-cover. Applied Ocean Research 32(3): 358-366. DOI: 10.1016/j.apor.2009.11.002

Das D, Sahu M (2021) Wave radiation by a sphere in three-layer fluid. Applied Ocean Research 107(2): 102-492. DOI: 10.1016/j.apor.2020.102492

Das D, Thakur N (2013) Wave scattering by a sphere submerged in uniform finite depth water with an ice-cover. Marine Structure 30: 63-73. DOI: 10.1016/j.marstruc.2012.11.001

Das D, Thakur N (2014) Wave scattering by a sphere submerged in a two-layer fluid with an ice-cover. International J Appl Math Engng Sci 8: 45-63. DOI: 10.1007/978-81-322-2547-8_17

Evans DV, Linton CM (1989) Active devices for the radiation of wave intensity. Applied Ocean Research 11(1): 26-32. DOI:10.1016/0141-1187(89)90004-7

Fernandez R, Parra RE, Milosevic Z, Dominguez S, Rossi C (2018) Design, modeling and control of a spherical autonomous underwater vehicle for mine exploration. IEEE/RSJ International Conference on Intelligent Robots and Systems (IROS), 1513-1519. DOI: 10.1109/IROS.2018.8594016

Gu Y, Ding B, Sergiienko NY, Cazzolato BS (2021) Power maximising control of a heaving point absorber wave energy converter. IET Renew. Power Gener 113. DOI: 10.1049/rpg2.12252

Havelock TH (1955) Waves due to a floating sphere making periodic heaving oscillations. Proc R Soc Lond A 231: 1-7. DOI: 10.1098/rspa.1955.0152

Linton CM (1991) Radiation and diffraction of water waves by a submerged sphere in finite depth. Ocean Engng 18(1-2): 61-74. DOI: 10.1016/0029-8018(91)90034-N

Linton CM, McIver M (1995) The interaction of waves with horizontal cylinders in two-layer fluids. J Fluid Mech 304: 213-229. DOI: 10.1017/S002211209500440X

Liu S, He G, Wang Z, Luan Z, Zhang Z, Wang W, Gao Y (2020) Resistance and flow field of a submarine in a density stratified fluid. Ocean Engng 217: 107934. DOI: 10.1016/j.oceaneng.2020.107934

Michallet H, Dias F (1999) Non-linear resonance between short and long waves. Proc 9th Inti Offshore and Polar Engineering Conference, 193-198

Mondal R, Sahoo T (2014) Wave structure interaction problems in three-layer fluid. *Z* Angew Math Phys 65(2): 349-375. DOI: 10.1007/s00033-013-0368-3

Sahu M, Das D (2021) Hydrodynamic forces on a submerged circular cylinder in two-layer fluid with an ice-cover. J Univ Shan Sci Tech 23: 282-294

Samayam S, Leontini J, Manasseh R, Sannasiraj SA, Sundar V (2021) Three-dimensional direct numerical simulation of flow induced by an oscillating sphere close to a plane boundary. Physics of Fluids 33(9): 97-106. DOI: 10.1063/5.0065651

Srokosz MA (1979) The submerged sphere as an absorber of wave power. Physics of Fluids 95(4): 717-741. DOI: 10.1017/S002211207900166X

Taylor GI (1931) Effect of variation in density on the stability of superposed streams of fluid. Proc Royal Soc Lond Ser A 132 (820): 717-741. DOI: 10.1098/rspa.1931.0115

Ursell F (1950) Surface waves on deep water in the presence of a submerged circular cylinder. I. Proc. Camb. Phil. Soc 46(1): 141-152. DOI: 10.1017/S0305004100025561

Wang C, Xu D, Gao J, Tan J, Zhou Z (2021) Numerical study of surface thermal signatures of lee waves excited by moving underwater sphere at low Froude number. Ocean Engng 235(3): 109314. DOI: 10.1016/j.oceaneng.2021.109314

Wu GX, Eatock Taylor R (1987) The exciting force on a submerged spheroid in regular waves. J Fluid Mech 182: 411-426. DOI: 10.1017/S0022112087002386

Wu GX, Eatock Taylor R (1989) On the radiation and diffraction of surface waves by submerged spheroids. J Ship Res 32(2): 84-92. DOI: 10.5957/jsr.1989.33.2.84